

pubs.acs.org/macroletters Letter

Strategy for Synthesis of Statistically Sequence-Controlled Uniform PLGA and Effects of Sequence Distribution on Interaction and Drug Release Properties

Jin Yoo, Dhushyanth Viswanath, and You-Yeon Won*



Cite This: ACS Macro Lett. 2021, 10, 1510–1516



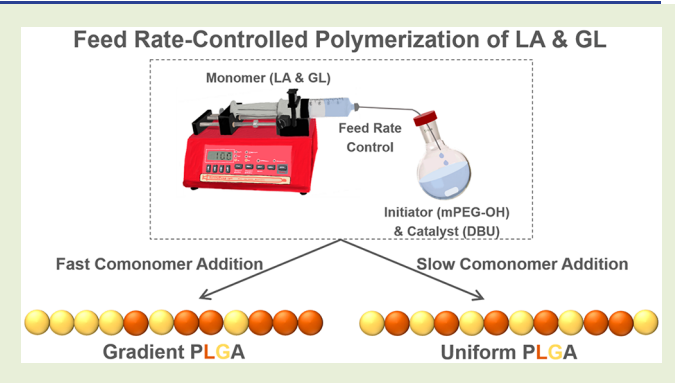
ACCESS

Metrics & More

Article Recommendations

Supporting Information

ABSTRACT: Extensive studies have been conducted to elucidate the effects of such parameters as molecular weight, polydispersity, and composition on the controlled release properties of poly(D,L-lactic-co-glycolic acid) (PLGA). However, studies dealing with the effect of monomer sequence distribution have been sparse mainly because of the difficulty of precisely controlling the monomer sequence in PLGA. Herein, we present a semibatch copolymerization strategy that enables the production of statistically sequence-controlled "uniform PLGA" polymers through control of the rate of comonomer addition. Using this method, a series of PEG—PLGA samples having a comparable molecular weight and composition but different sequence distributions (uniform vs gradient) were prepared. The properties of these materials (PEG



crystallization/melting, hygroscopicity, aqueous sol—gel transition, drug release kinetics) were found to significantly vary, demonstrating that sequence control only at the statistical level still significantly influences the properties of PLGA. Most notably, uniform PLGA exhibited the more sustained drug release behavior compared to gradient PLGA.

The synthesis of monodisperse, high molecular weight (MW) PLGA has been a topic of interest because of its usefulness for various biomedical applications. Ring-opening polymerization (ROP) of lactide (LA) and glycolide (GL) requires a catalyst to make the reaction proceed at a reasonable rate. Metal catalysts are common choices with tin being the most widely used. With a tin catalyst, LA and GL undergo polymerization by the coordination—insertion mechanism. This chemistry enables high MW PLGA (>100 kDa) to be produced within minutes to hours at not-too-inconvenient temperatures (130–200 °C). MWs and polydispersities are controlled by the propagation-to-initiation rate ratio and the extent of transesterification. Transesterification is promoted at elevated temperatures (>130 °C)⁴ and results in a broadening of the MW distribution.

Another inconvenient aspect of the ROP of LA and GL is the large difference in reactivity between the two monomers; for tin-catalyzed ROP reactions, the reactivity ratios are $r_{\rm LA}\cong 0.2$ and $r_{\rm GL}\cong 2.8$ at 200 °C.⁶ As a result, a conventional batch copolymerization reaction produces a gradient PLGA having long sequences of GL near the initiating end and long sequences of LA toward the opposite end of a chain.

Recently, organic catalysts^{7,8} have emerged as alternatives to metal catalysts. Organic catalysts enable the ROP of LA/GL to be effected at ambient temperature, thereby without transesterification reactions.⁹ However, under organic catalysts, the

disparity of the reactivities becomes exacerbated 10 ($r_{\rm LA}\cong 3.37\times 10^{-2}$ and $r_{\rm GL}\cong 13.6$ in the 1,8-diazabicyclo[5.4.0]undec-7-ene(DBU)-catalyzed process at room temperature 11). This renders it impossible to produce PLGA products using a batch process because gradient PLGA polymers containing long GL sequences are not soluble in most organic solvents. 12 To address this limitation, researchers have proposed a semibatch copolymerization strategy (a constant-rate GL addition method). 13,14 However, this method is still incapable of producing a sequence uniform PLGA copolymer. 11 A semibatch process having a varying-rate monomer addition is required to produce the desired uniform PLGA architecture. 15 However, it is difficult to execute this concept, especially when DBU is used as the catalyst, because the reactivity ratios differ greatly between LA and GL. 11

Recently, Meyer and co-workers demonstrated a method to deterministically control the repeat unit sequences in PLGA. Their "segmer assembly polymerization" method involves condensation reactions of "segmers" containing predesigned

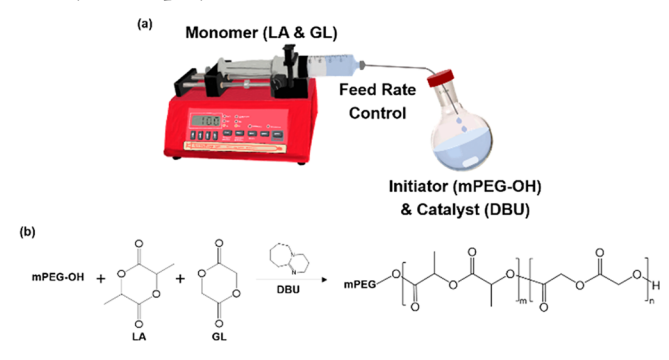
Received: October 12, 2021 Accepted: November 12, 2021



sequences of lactate and glycolate units. However, there are potential disadvantages of this method, which include (i) additional steps needed to prepare segmers, and (ii) higher polydispersity indices (PDI)¹⁷ and (iii) lower MWs achievable¹⁸ relative to ROP methods. Ding and co-workers used transesterification reactions as a means of increasing the randomness of the PLGA sequence;¹⁹ PLGA-PEG-PLGA materials were synthesized with a tin catalyst at two different temperatures (130 vs 160 °C). The copolymer prepared at the higher temperature showed a more uniform monomer distribution because of a greater level of transesterification. However, this method does not allow precise control of the sequence and also accompanies a broadening of the MW distribution.

In this Letter, we demonstrate an alternative approach for producing uniform PLGA products with narrow MW distributions via semibatch ROP. In this approach, a mixture of LA and GL is continuously fed into the reactor at a constant rate, unlike the previous approach in which only the more reactive GL is continuously added. In our case, the sequence distribution is controlled by the comonomer feed rate; so this method is called "feed rate-controlled polymerization (FRCP)". The idea is that the disparity in monomer reactivities becomes unimportant in the slow comonomer feed limit, that is, when the feed rate is slower than the polymerization rates. One can imagine the extreme situation, where small amounts of LA and GL molecules are either in one feed stream (Scheme 1) or in separate streams, added to the

Scheme 1. (a) Schematic Depiction of the Feed Rate Controlled Polymerization (FRCP) Process;^a (b) DBU-Catalyzed Copolymerization of LA and GL



"Both lactide (LA) and glycolide (GL) monomers (either together as a mixture or in separate feed streams) are continuously fed into the reactor at a constant rate.

reactor each time at sufficiently long intervals between additions; in this case, the copolymer sequence is not controlled by the inherent reactivities of the monomers, but instead by the rate(s) of their addition. In reality, the smallest amount of monomers that can be added to the reactor at each addition step is limited by the size of the droplet of the comonomer solution (Scheme 1); therefore, the PLGA produced by the FRCP must possess some level of sequence gradient at local scales, although on a global scale, the monomer distribution must be uniform.

To demonstrate this FRCP concept, a series of $PEG_{5.0k}$ - $PL_{2.5k}G_{2.5k}A$ materials were synthesized under different comonomer feed rate and polymerization rate conditions; the polymerization rate was controlled by DBU (catalyst) concentration. Briefly, 10 mL of a comonomer solution

containing 116 mM LA and 144 mM GL in dichloromethane (DCM) was injected at various rates (0.05-0.3 mL/min) into the reactor that initially contained 5 mL of an initiator/catalyst solution (11.2 mM mPEG-OH and 11-33 mM DBU in DCM). The polymerization was run for the time needed to complete the comonomer injection and then terminated by adding benzoic acid. As summarized in Table 1 (runs 1-5), at fast monomer feed rates and low DBU concentrations, the reaction mixture turned opaque due to the generation of (PEG-)PLGA chains containing long GL sequences and their precipitation; at slower monomer feed rates/higher DBU concentrations, the reaction mixture remained transparent throughout the reaction, suggesting more uniform sequence characteristics for the PLGA products. The resultant PEG-PLGA was characterized by ¹H NMR to determine its MW (Figure S1). As shown in Table 1, as the monomer feed rate was increased (runs 4 and 5) or the DBU concentration was decreased (run 1), the PLGA block MW decreased because of the precipitation of the growing chains, which limited the polymerization conversion.

Similar experiments were also performed targeting $PEG_{5.0k}$ - $PL_{5.0k}G_{5.0k}$ - $PL_{7.5k}G_{2.5k}$ A microstructures (runs 6 and 8–11, respectively, in Table 1). For the $PEG_{5.0k}$ - $PL_{7.5k}G_{2.5k}$ A experiments, larger amounts of DBU had to be added in order to obtain a high monomer conversion because the less reactive LA was the majority monomer component (run 10). Overall, all qualitative trends were the same as those observed in the previous $PEG_{5.0k}$ - $PL_{2.5k}G_{2.5k}$ A case.

The PEG_{5.0k}-PL_{5.0k}G_{5.0k}A samples (runs 6 and 7 in Table 1) were chosen for detailed microstructural investigation. In addition to the products of Runs 6 and 7 (named, respectively, as OLG2 and OLG3 in Table 2), one additional sample (OLG1) was prepared at a slower feed rate (0.03 mL/min) for this study. As indicated in Table 2, for the synthesis of OLG1, DBU was injected three times (20 μ L of DBU injected at every 2 h) to obtain a high monomer conversion because of the long reaction time (~6 h at the 0.03 mL/min comonomer addition rate) and the deactivation of DBU over time.²⁰ The sequence properties of OLG1, OLG2, and OLG3 were characterized by 13C NMR.^{21,22} The signals from the carbonyl carbons were analyzed to determine the cumulative lactyl-lactyl, lactylglycolyl, glycolyl-lactyl, and glycolyl-glycolyl diad concentrations (I_{LL}, I_{LG}, I_{GL}) and I_{GG} , respectively). ¹⁴ The I_{LL} and I_{LG} data were obtained using hexafluoroisopropanol as the solvent (Figure 1a), 14,23 and the I_{GL} and I_{GG} data used were obtained using DMSO- d_6 as the solvent (Figure S3).²⁴ The cumulative number-average lactate/glycolate sequence lengths $(\overline{L_L}$ and $\overline{L_G}$, respectively) were calculated using the following equations (derivations given in the Supporting Information (SI)):

$$\overline{L_L} = 2\frac{I_{LL}}{I_{LG}} + 2; \ \overline{L_G} = 2\frac{I_{GG}}{I_{GL}} + 2$$
 (1)

As shown in Table 2, the results confirm that a slower comonomer feed rate gives shorter average LA/GL sequence lengths and thus a more uniform sequence distribution.

The molecular characteristics of the copolymers produced by the FRCP method (OLG1, OLG2, and OLG3) were also compared with those of a commercial PEG_{5.0k}-PL_{5.0k}G_{5.0k}A product synthesized with a tin catalyst (AK010, PolySciTech). As shown in Figure S3 (1 H NMR), the chemical composition of AK010 (LA/GL \cong 50:50) is similar to that of our polymers. The number-average lactate/glycolate sequence lengths of

Table 1. Summary of PEG-PLGA Polymers Synthesized Using the FRCP Method under Different Comonomer Feed Rate and DBU Concentration Conditions^a

run No.	polymer target	feed rate (mL/min)	$[DBU]_o$ (mM)	product in DCM	polymer product ^c	
1	$PEG_{5.0k}\text{-}PL_{2.5k}G_{2.5k}A$	0.10	11.1	opaque	$PEG_{5.0k}\text{-}PL_{0.29k}G_{1.2k}A$	
2	$PEG_{5.0k}\text{-}PL_{2.5k}G_{2.5k}A$	0.05	33.5	transparent	$PEG_{5.0k}$ - $PL_{1.9k}G_{2.1k}A$	
3 ^b	$PEG_{5.0k}$ - $PL_{2.5k}G_{2.5k}A$	0.10	33.5	transparent	$PEG_{5.0k}-PL_{2.0k}G_{2.0k}A$	
4	$PEG_{5.0k}\text{-}PL_{2.5k}G_{2.5k}A$	0.20	33.5	translucent	$PEG_{5.0k}$ - $PL_{1.9k}G_{2.0k}A$	
5	$PEG_{5.0k}\text{-}PL_{2.5k}G_{2.5k}A$	0.30	33.5	opaque	$PEG_{5.0k}$ - $PL_{1.7k}G_{2.0k}A$	
6^{b}	$PEG_{5.0k}$ - $PL_{5.0k}G_{5.0k}A$	0.05	33.5	transparent	$PEG_{5.0k}-PL_{4.3k}G_{4.6k}A$	
7	$PEG_{5.0k}$ - $PL_{5.0k}G_{5.0k}A$	0.10	33.5	opaque	$PEG_{5.0k}$ - $PL_{4.1k}G_{4.8k}A$	
8	$PEG_{5.0k}\text{-}PL_{7.5k}G_{2.5k}A$	0.03	33.5	transparent	$PEG_{5.0k}$ - $PL_{3.8k}G_{1.7k}A$	
9	$PEG_{5.0k}\text{-}PL_{7.5k}G_{2.5k}A$	0.05	33.5	transparent	$PEG_{5.0k}$ - $PL_{5.6k}G_{2.1k}A$	
10 ^b	$PEG_{5.0k}$ - $PL_{7.5k}G_{2.5k}A$	0.05	55.8	transparent	$PEG_{5.0k}-PL_{6.4k}G_{2.0k}A$	
11	$PEG_{5.0k}-PL_{7.5k}G_{2.5k}A$	0.05	89.3	transparent	$PEG_{5.0k}-PL_{5.5k}G_{2.0k}A$	

^aThe reaction conditions were as follows: for all runs, the volume of comonomer feed solution injected into the reactor = 10 mL, the initial volume of initiator/catalyst solution in the reactor = 6.0 mL, [mPEG-OH]_o = 11.2 mM (reactor), solvent = DCM (for both comonomer and initiator/catalyst solutions), T = 25 °C; for PEG_{5.0k}-PL_{2.5k}G_{2.5k}A, [LA]_o = 116 mM (feed), [GL]_o = 144 mM (feed); for PEG_{5.0k}-PL_{5.0k}G_{5.0k}A, [LA]_o = 232 mM (feed), [GL]_o = 289 mM (feed); for PEG_{5.0k}-PL_{7.5k}G_{2.5k}A, [LA]_o = 349 mM (feed), [GL]_o = 144 mM (feed). ^bItalicized entries represent the best among tested conditions identified for producing the respective target PEG–PLGA products. ^cBased on ¹H NMR.

Table 2. Cumulative Number-Average Lactate and Glycolate Sequence Lengths ($\overline{L_L}$ and $\overline{L_G}$, Respectively) for PEG_{5.0k}-PL_{5.0k}G_{5.0k}A Polymers Synthesized under Different Comonomer Feed Rate Conditions

polymer ID	feed rate (mL/min)	$[DBU]_o (mM)$	polymer product ^a	I_{LL}/I_{LG}^{b}	$\overline{L_L}^c$	I_{GG}/I_{GL}^{d}	$\overline{L_G}^c$
OLG1	0.03	22.3×3^{e}	$PEG_{5.0k}$ - $PL_{5.2k}G_{5.0k}A$	1.48	4.96	1.89	5.78
OLG2	0.05	33.5	$PEG_{5.0k}$ - $PL_{4.3k}G_{4.6k}A$	1.78	5.56	2.06	6.12
OLG3	0.10	33.5	$PEG_{5.0k}-PL_{4.1k}G_{4.8k}A$	1.74	5.48	2.58	7.16

"Number-average molecular weight values were determined by ¹H NMR (Figure S2). ^bDetermined by ¹³C NMR using hexafluoroisopropanol as the solvent (Figure 1a). ^cCalculated using eq 1. ^dDetermined by ¹³C NMR using DMSO- d_6 as the solvent (Figure S2). ^{ea}× 3" denotes that 3 doses of DBU (20 μ L of DBU per injection) were added to the reactor (at the beginning and every 2 h thereafter).

AK010 were $\overline{L_L} \cong 4.76$ and $\overline{L_G} \cong 5.98$, respectively (Figure S4). In terms of sequence uniformity, AK010 is not better than OLG1 (Table 2), although in the AK010 case, both the less disparate reactivities of LA and GL with the tin catalyst and the transesterification that occurred during the polymerization enhanced the uniformity of the sequence distribution. GPC data show that the FRCP products are more monodisperse (PDI $\cong 1.1-1.2$) than AK010 (PDI $\cong 1.8$; Figure S5).

In the remainder of this paper, we report on the investigation of the effects of sequence distribution on the structural and interaction properties of PEG-PLGA polymers. Figure 1b shows differential scanning calorimetry (DSC) profiles of OLG1, OLG2, and OLG3; the DSC profile of a mPEG_{5.0k}-OH homopolymer is presented in Figure S6. The melting temperatures of the PEG_{5.0k}-PL_{5.0k}G_{5.0k}A copolymers $(T_{\rm m} \cong 40-52 \, {}^{\circ}\text{C})$ were significantly lower than that of mPEG_{5.0k}-OH ($T_{\rm m} \cong 67$ °C). Among the three copolymers, the $T_{\rm m}$ decrease was greatest for OLG1 ($T_{\rm m} \cong 40~{\rm ^{\circ}C}$), followed by OLG2 ($T_{\rm m} \cong 44~^{\circ}{\rm C}$) and then by OLG3 ($T_{\rm m} \cong 50$ °C). This trend reflects the fact that from OLG3 to OLG2 to OLG1, the monomer sequence gradient decreases, particularly near the junction point between the PEG and PLGA blocks. According to the Gibbs-Thomson equation,²⁵ the melting temperature depression ($\Delta T_{\rm m} \equiv T_{\rm m}^{\infty} - T_{\rm m}$, where $T_{\rm m}^{\infty}$ is the equilibrium melting temperature) is proportional to the interfacial tension (γ) between the crystalline and amorphous phases. The PEG crystal-melt interfacial tension (γ) is influenced by the miscibility between the PEG and PLGA blocks. Based on the polymer solubility parameters ($\delta_{\text{PEG}}\cong$ 19.2 (J/cc)^{1/2}, $\delta_{PLA} \cong 21.4$ (J/cc)^{1/2}, and $\delta_{PGA} \cong 23.8$ (J/cc)^{1/2})²⁶⁻²⁸ and the monomer volume of PEG ($\nu_{PEG} \cong 39.0$ cc/mol), the Flory—Huggins parameters are estimated to be $\chi_{\rm PEG/PLA} \cong 0.18$ and $\chi_{\rm PEG/PGA} \cong 0.53$, respectively, for the PEG/PLA and PEG/PGA combinations at 25 °C, which implies that PEG interacts more favorably with PLA than with PGA. OLG1 contains the least amount of GL sequences near the block junction, and therefore the greatest amount of PLGA segments would intrude into the fold region of the semicrystalline PEG domain of the neat OLG1 material; OLG3 would be the opposite end of this comparison. Therefore, OLG1, followed by OLG2 and OLG3, should exhibit the highest γ and thus the lowest $T_{\rm m}$ (the greatest $\Delta T_{\rm m}$) as observed experimentally. This trend observed in terms of $\Delta T_{\rm m}$ (Figure 1b) also agrees with the trend in the degree of crystallinity (Table S1); as the crystalline fraction decreases, the $T_{\rm m}$ decreases.

A separate moisture absorption experiment was performed to confirm the crystallinity trend. The OLG1, OLG2, and OLG3 samples were placed within a humidified chamber (85% relative humidity) at ambient temperature for 2 days. Afterward, the amounts of moisture absorbed by the polymers were measured by thermogravimetric analysis (TGA). As shown in Figure 1c (weight losses between about 60 and 100 °C), OLG1 had the greatest moisture content, followed by OLG2, and OLG3 had the lowest moisture content. These results agree with the DSC results (OLG1 > OLG2 \geq OLG3 in the amorphous fraction; Figure 1b and Table S1).

The effects of PLGA monomer sequence on PEG structures were evident even in aqueous self-assembly situations. Micelle solutions of OLG1, OLG2, and OLG3 were prepared by direct dissolution of the polymers (0.5% by weight) in Milli-Q water (Figures S7 and S8). Differences in the PEG corona properties

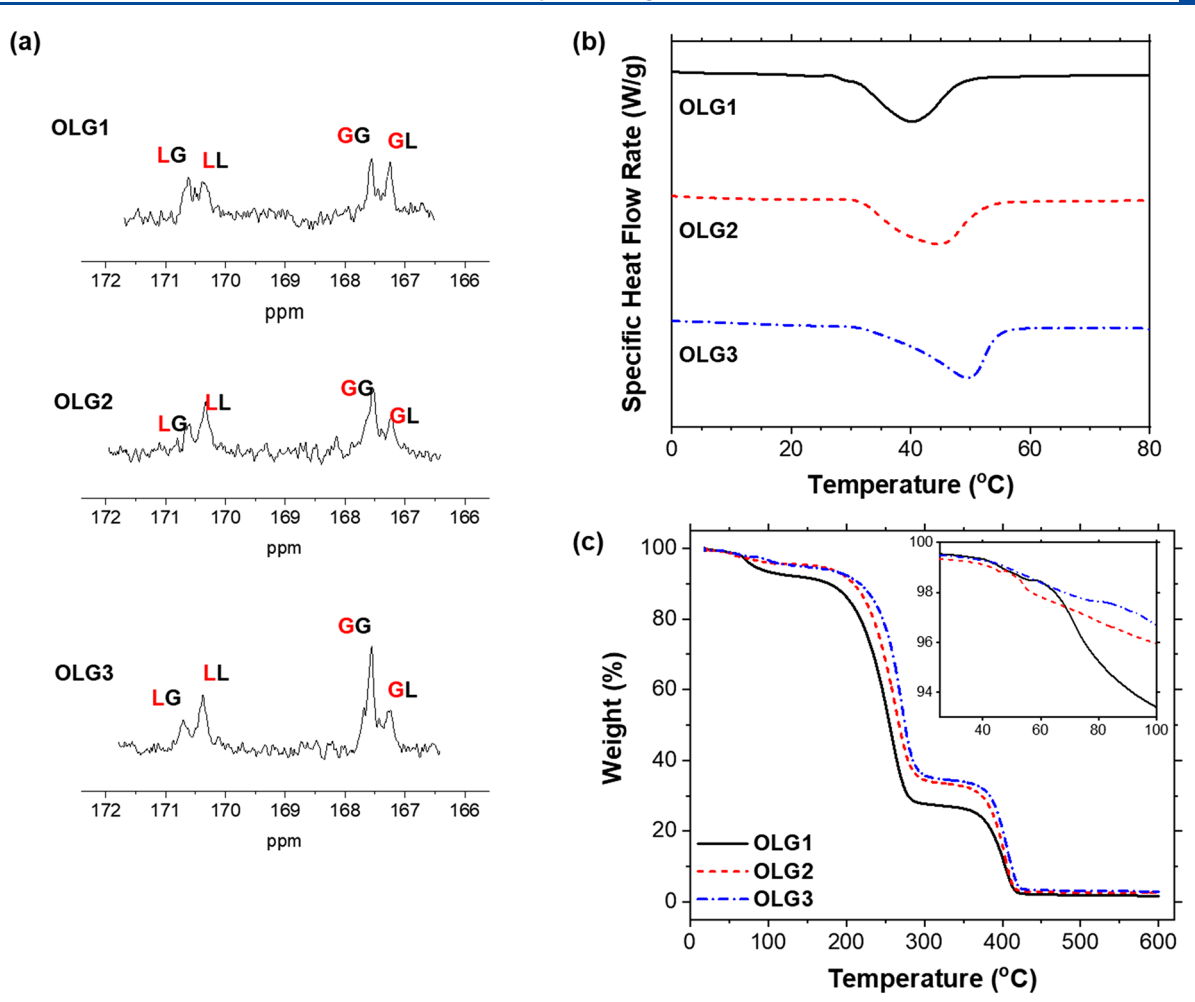


Figure 1. (a) 13 C NMR spectra (carbonyl resonances) of the PEG_{5.0k}-PL_{5.0k}G_{5.0k}A polymers produced under three different monomer feed rate conditions (named OLG1, OLG2, and OLG3). See Table 2 for the monomer feed rates used and the molecular weight/monomer sequence length characteristics and Figure S5 for the polydispersity indices (PDIs) of these polymers. The NMR spectra were obtained using a coaxial tube with the polymer/hexafluoroisopropanol solution placed in the outer tube and blank DMSO- d_6 in the inner tube. (b) DSC and (c) TGA traces for OLG1, OLG2, and OLG3.

of these micelles were examined by investigation of the interactions of these micelles with laponite (clay) nanoparticles. As shown in Figure S9, all three PLGA-PEG micelles formed gels with laponite at elevated temperatures. The OLG1/laponite system exhibited the highest sol—gel transition temperature, followed by the OLG2/laponite and then OLG3/laponite systems, which is consistent with a previous report that PLGA-PEG-PLGA triblock copolymers with longer LA/GL sequences exhibit lower gelation temperatures; ¹⁹ detailed discussions of these results are presented in the SI.

We explored how the PLGA sequence distribution affects the drug release properties of PEG-PLGA. Paclitaxel (PTX)-loaded PEG-PLGA nanoparticles ("PEG-PLGA/PTX NPs"; having a hydrodynamic diameter of ~700 nm) were prepared from OLG1, OLG2, and OLG3 using the emulsion-evaporation procedure.³¹ The size and drug loading characteristics of the resultant PEG-PLGA/PTX NPs are summarized in Figure 2a and Table S2. Scanning electron microscopy (SEM) images (Figure 2a) show that all PEG-PLGA/PTX NPs have a spherical shape and nonporous surfaces. In all formulations, single holes of ~150 nm diameter were observed in about 10% of the particles (created due to the evaporation flux of DCM).³² Transmission electron microscopy (TEM) images

(Figure S10) confirmed that these PEG-PLGA/PTX NPs are open hollow spheres.

The PTX release kinetics of the three NP formulations were characterized at 37 °C. As shown in Figure 2b, the PTX release was the fastest with OLG3 (\sim 50% released immediately and \sim 80% within 48 h). The release kinetics were comparable between OLG1 and OLG2, and they were much slower than that of OLG3 (only \sim 30% released during the first 48 h in both the OLG1 and OLG2 cases). We believe that this dramatic difference in drug release kinetics was also caused by the different sequence characteristics. Based on the solubility parameter values of PLA and PGA ($\delta_{\rm PLA}\cong21.4~(\rm J/cc)^{1/2}$, and $\delta_{\rm PGA}\cong23.8~(\rm J/cc)^{1/2})$ and that of PTX ($\delta_{\rm PTX}\cong25.2~(\rm J/cc)^{1/2}),^{26,27}$ the Flory–Huggins parameters are estimated to be $\chi_{\rm PLA/PTX}\cong2.23~{\rm for}~{\rm PLA/PTX}~{\rm mixtures}~{\rm and}~\chi_{\rm PGA/PTX}\cong0.24~{\rm for}~{\rm PGA/PTX}~{\rm mixtures}~{\rm at}~25~{\rm °C};~{\rm PTX}~{\rm is}~{\rm more}~{\rm miscible}~{\rm with}~{\rm PGA}~{\rm than}~{\rm with}~{\rm PLA}.$ Therefore, in PEG-PLGA NPs, PTX will partition more in the GL-rich region than in the LA-rich region.

The hydrophobic core domain of an OLG3/PTX NP must have a gradient in composition; the region near the aqueous-core interface is rich with GL units, whereas the deeper side of the core is primarily composed of LA units. In the OLG3 case, because of its affinity to GL, PTX is more concentrated in the

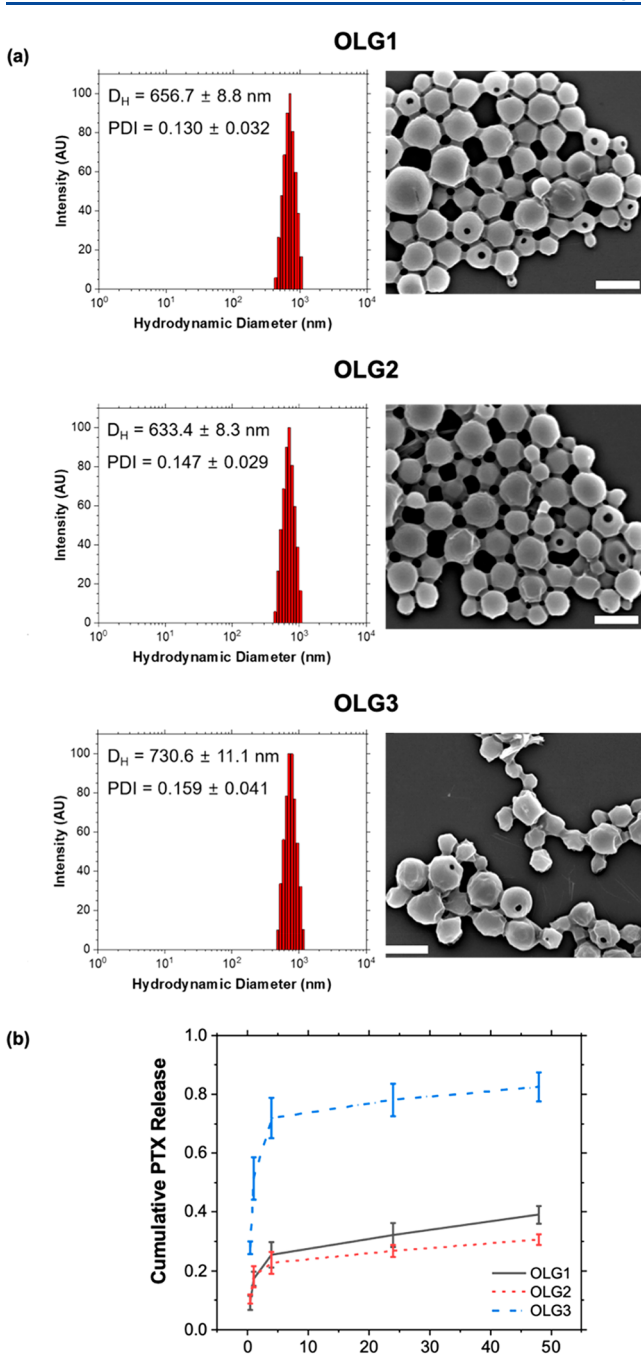


Figure 2. (a) DLS histograms (left) and SEM images (right) of PTX-loaded PEG-PLGA nanoparticles (PEG-PLGA/PTX NPs) produced via an emulsion-evaporation process. DLS was performed on 0.05% (by weight) suspensions of PEG-PLGA/PTX NPs in Milli-Q water. SEM was performed on dried specimens. Scale bars represent 1 μ m. (b) Kinetics of PTX release from PEG-PLGA/PTX NPs (shown in (a)) in a pH 7.4 buffer containing 20 mg/mL Tween 80 surfactant (to accelerate the PTX release rate) at 37 °C.

Time (h)

peripheral region of the core domain, and as a result, PTX is released faster from the OLG3/PTX NPs than the other two systems (OLG1/PTX and OLG2/PTX NPs); in the latter cases, a more uniform PLGA sequence distribution causes PTX to be more homogeneously distributed within the core domain and thus to be released from it slower. These explanations are schematically summarized in Figure 3.

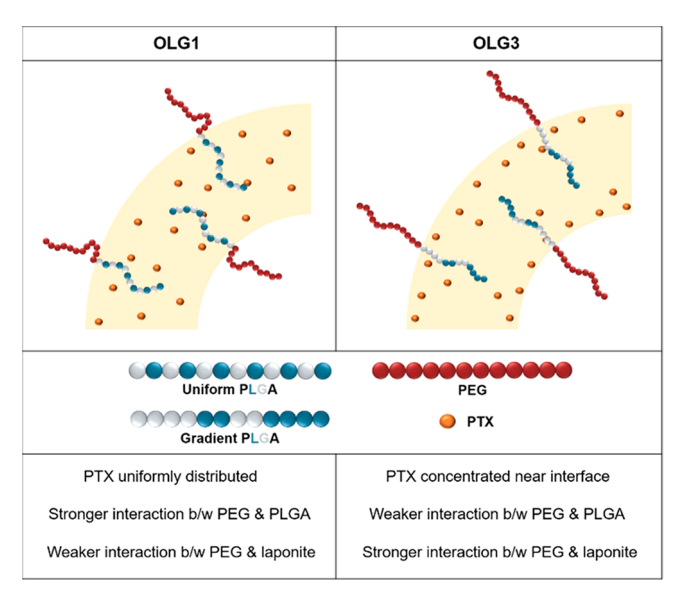


Figure 3. Summary of the findings of this study, that is, the effects of PLGA monomer sequence distribution on the conformational and interaction properties of aqueous PEG-PLGA self-assemblies.

In summary, we have developed a new, feed rate-controlled polymerization (FRCP) method, in which the LA + GL mixture is continuously fed into the ROP at a sufficiently slow rate, so that the disparity of the reactivities of LA and GL does not bias the monomer distribution of the copolymer product, and as a result, "uniform PLGA" polymers can be produced. Using this FRCP method, monodisperse PEG-PLGA block copolymers (OLG1, OLG2, and OLG3) with varying degrees of sequence uniformity have been prepared and used to demonstrate the effects of LA/GL sequence distribution on the properties of the copolymers. As summarized in Figure 3, the uniform LA/GL sequence distribution in PEG-PLGA renders the PEG chains less crystallizable in the neat state and less interactive with water and mineral surfaces in the aqueous selfassembled state. When PTX is loaded, the sequence uniformity forces the PTX molecules to be more homogeneously distributed within the PLGA domain, which suppresses the burst release of PTX and causes the release process to be more sustained. Sequence control might hold the key to solving the long-standing challenge associated with PLGA microencapsulation, a hard-to-predict, initial burst drug release behavior.³³ The FRCP method offers a facile route for the production of "uniform PLGA" materials for controlled release applications.

ASSOCIATED CONTENT

3 Supporting Information

The Supporting Information is available free of charge at https://pubs.acs.org/doi/10.1021/acsmacrolett.1c00637.

Experimental procedures; Supplemental figures (¹H/¹³C NMR spectra, GPC traces, DSC thermograms, optical photographs, TEM micrographs, DLS histograms); Supplemental tables (areas under the DSC endothermic peaks, size/composition characteristics of PEG-PLGA/PTX NPs) (PDF)

AUTHOR INFORMATION

Corresponding Author

You-Yeon Won – Davidson School of Chemical Engineering, Purdue University, West Lafayette, Indiana 47907, United

States of America; Purdue University Center for Cancer Research, Purdue University, West Lafayette, Indiana 47906, United States of America; oorcid.org/0000-0002-8347-6375; Email: yywon@purdue.edu

Authors

Jin Yoo – Davidson School of Chemical Engineering, Purdue University, West Lafayette, Indiana 47907, United States of America; orcid.org/0000-0002-6627-6785

Dhushyanth Viswanath – Davidson School of Chemical Engineering, Purdue University, West Lafayette, Indiana 47907, United States of America

Complete contact information is available at: https://pubs.acs.org/10.1021/acsmacrolett.1c00637

Author Contributions

All authors have contributed to the writing and approved the manuscript being submitted.

Notes

The authors declare no competing financial interest.

ACKNOWLEDGMENTS

The authors thank the U.S. National Science Foundation (NSF) for providing financial support for this research (CBET-1803968) and the Ministry of Education of the Korean Government for the NRF Postdoctoral Fellowship granted to J.Y. (2020R1A6A3A03037188). The authors also acknowledge support from the Purdue University Center for Cancer Research (PCCR) via an NIH NCI Grant (P30 CA023168), which supports the campus-wide NMR shared resources that were utilized in this work.

■ REFERENCES

- (1) Kaihara, S.; Matsumura, S.; Mikos, A. G.; Fisher, J. P. Synthesis of poly(L-lactide) and polyglycolide by ring-opening polymerization. *Nat. Protoc.* **2007**, 2 (11), 2767–71.
- (2) Dechy-Cabaret, O.; Martin-Vaca, B.; Bourissou, D. Controlled Ring-Opening Polymerization of Lactide and Glycolide. *Chem. Rev.* **2004**, *104* (12), 6147–6176.
- (3) Yu, Y.; Fischer, E. J.; Storti, G.; Morbidelli, M. Modeling of Molecular Weight Distribution in Ring-Opening Polymerization of l,l-Lactide. *Ind. Eng. Chem. Res.* **2014**, 53 (18), 7333–7342.
- (4) Gallardo, A.; Marcos-Fernández, A.; Egri, S.; Lebrón, R.; Piskin, E. MALDI-TOF Analysis of the Secondary Processes Occurring During the Ring Opening Polymerization of Caprolactone Initiated by HEMA. *Int. J. Polym. Anal. Charact.* **2008**, *13* (2), 83–94.
- (5) Zhang, X.; Jones, G. O.; Hedrick, J. L.; Waymouth, R. M. Fast and selective ring-opening polymerizations by alkoxides and thioureas. *Nat. Chem.* **2016**, *8* (11), 1047–1053.
- (6) Gilding, D.K.; Reed, A.M. Biodegradable polymers for use in surgery-polyglycolic/poly(lactic acid)homo- and copolymers: 1. *Polymer* 1979, 20 (12), 1459–1464.
- (7) Lohmeijer, B. G. G.; Pratt, R. C.; Leibfarth, F.; Logan, J. W.; Long, D. A.; Dove, A. P.; Nederberg, F.; Choi, J.; Wade, C.; Waymouth, R. M.; Hedrick, J. L. Guanidine and Amidine Organocatalysts for Ring-Opening Polymerization of Cyclic Esters. *Macromolecules* **2006**, 39 (25), 8574–8583.
- (8) Chuma, A.; Horn, H. W.; Swope, W. C.; Pratt, R. C.; Zhang, L.; Lohmeijer, B. G. G.; Wade, C. G.; Waymouth, R. M.; Hedrick, J. L.; Rice, J. E. The Reaction Mechanism for the Organocatalytic Ring-Opening Polymerization of l-Lactide Using a Guanidine-Based Catalyst: Hydrogen-Bonded or Covalently Bound? *J. Am. Chem. Soc.* 2008, 130 (21), 6749–6754.
- (9) Dove, A. P. Organic Catalysis for Ring-Opening Polymerization. *ACS Macro Lett.* **2012**, *1* (12), 1409–1412.

- (10) Kemo, V. M.; Schmidt, C.; Zhang, Y.; Beuermann, S. Low Temperature Ring-Opening Polymerization of Diglycolide Using Organocatalysts with PEG as Macroinitiator. *Macromol. Chem. Phys.* **2016**, 217 (7), 842–849.
- (11) Patil, S. M.; Yoo, J.; Won, Y.-Y. The Kinetics of the DBU-Catalyzed Copolymerization of Lactide and Glycolide. *Ind. Eng. Chem. Res.* **2021**, *60* (41), 14685–14700.
- (12) Park, K.; Skidmore, S.; Hadar, J.; Garner, J.; Park, H.; Otte, A.; Soh, B. K.; Yoon, G.; Yu, D. J.; Yun, Y.; Lee, B. K.; Jiang, X. H.; Wang, Y. Injectable, long-acting PLGA formulations: Analyzing PLGA and understanding microparticle formation. *J. Controlled Release* **2019**, 304, 125–134.
- (13) McGrath, J. E. Chain reaction polymerization. *J. Chem. Educ.* **1981**, *58* (11), 844–861.
- (14) Qian, H.; Wohl, A. R.; Crow, J. T.; Macosko, C. W.; Hoye, T. R. A Strategy for Control of "Random" Copolymerization of Lactide and Glycolide: Application to Synthesis of PEG-b-PLGA Block Polymers Having Narrow Dispersity. *Macromolecules* **2011**, *44* (18), 7132–7140.
- (15) Austin, A. B. J. S., Rate Matched Copolymerization. U.S. Patent 6,828,393, Dec 7, 2004.
- (16) Li, J.; Rothstein, S. N.; Little, S. R.; Edenborn, H. M.; Meyer, T. Y. The effect of monomer order on the hydrolysis of biodegradable poly(lactic-co-glycolic acid) repeating sequence copolymers. *J. Am. Chem. Soc.* **2012**, *134* (39), 16352–9.
- (17) Washington, M. A.; Swiner, D. J.; Bell, K. R.; Fedorchak, M. V.; Little, S. R.; Meyer, T. Y. The impact of monomer sequence and stereochemistry on the swelling and erosion of biodegradable poly(lactic-co-glycolic acid) matrices. *Biomaterials* **2017**, *117*, 66–76.
- (18) Washington, M. A.; Balmert, S. C.; Fedorchak, M. V.; Little, S. R.; Watkins, S. C.; Meyer, T. Y. Monomer sequence in PLGA microparticles: Effects on acidic microclimates and in vivo inflammatory response. *Acta Biomater.* **2018**, *65*, 259–271.
- (19) Yu, L.; Zhang, Z.; Ding, J. Influence of LA and GA sequence in the PLGA block on the properties of thermogelling PLGA-PEG-PLGA block copolymers. *Biomacromolecules* **2011**, *12* (4), 1290–7.
- (20) Sherck, N. J.; Kim, H. C.; Won, Y. Y. Elucidating a Unified Mechanistic Scheme for the DBU-Catalyzed Ring-Opening Polymerization of Lactide to Poly(lactic acid). *Macromolecules* **2016**, *49* (13), 4699–4713.
- (21) Skidmore, S.; Hadar, J.; Garner, J.; Park, H.; Park, K.; Wang, Y.; Jiang, X. J. Complex sameness: Separation of mixed poly(lactide-coglycolide)s based on the lactide:glycolide ratio. *J. Controlled Release* **2019**, *300*, 174–184.
- (22) Fernandez, J.; Etxeberria, A.; Ugartemendia, J. M.; Petisco, S.; Sarasua, J. R. Effects of chain microstructures on mechanical behavior and aging of a poly(L-lactide-co-epsilon-caprolactone) biomedical thermoplastic-elastomer. *J. Mech. Behav. Biomed. Mater.* **2012**, *12*, 29–38.
- (23) Grijpma, D.W; Nijenhuis, A.J; Pennings, A.J Synthesis and hydrolytic degradation behaviour of high-molecular-weight L-lactide and glycolide copolymers. *Polymer* **1990**, *31* (11), 2201–2206.
- (24) Wang, L.; Venkatraman, S.; Gan, L. H.; Kleiner, L. Structure formation in injectable poly(lactide-co-glycolide) depots. II. Nature of the gel. *J. Biomed. Mater. Res.* **2005**, 72 (1), 215–22.
- (25) Han, C. C.; Shi, W.; Jin, J., Morphology and Crystallization of Crystalline/Amorphous Polymer Blends. In *Encyclopedia of Polymers and Composites*; Springer-Verlag: Berlin/Heidelberg, Germany, 2013; pp 1–19.
- (26) Agrawal, A.; Saran, A. D.; Rath, S. S.; Khanna, A. Constrained nonlinear optimization for solubility parameters of poly(lactic acid) and poly(glycolic acid)—validation and comparison. *Polymer* **2004**, 45 (25), 8603–8612.
- (27) Du, Z.; Zhang, Y.; Xu, H.; Lang, M. Functionalized Pluronic-b-poly(epsilon-caprolactone) based nanocarriers of paclitaxel: solubilization, antiproliferative efficacy and in vivo pharmaceutic kinetics. *J. Mater. Chem. B* **2015**, 3 (18), 3685–3694.

- (28) Özdemir, C.; Güner, A. Solubility profiles of poly(ethylene glycol)/solvent systems, I: Qualitative comparison of solubility parameter approaches. *Eur. Polym. J.* **2007**, 43 (7), 3068–3093.
- (29) Chu, B.; Zhang, L.; Qu, Y.; Chen, X.; Peng, J.; Huang, Y.; Qian, Z. Synthesis, characterization and drug loading property of Monomethoxy-poly(ethylene glycol)-poly(epsilon-caprolactone)-poly(D,L-lactide) (MPEG-PCLA) copolymers. Sci. Rep. 2016, 6, 34069.
- (30) Kim, H. C.; Choi, Y. H.; Bu, W.; Meron, M.; Lin, B.; Won, Y. Y. Increased humidity can soften glassy Langmuir polymer films by two mechanisms: plasticization of the polymer material, and suppression of the evaporation cooling effect. *Phys. Chem. Chem. Phys.* **2017**, *19* (16), 10663–10675.
- (31) Wadajkar, A. S.; Dancy, J. G.; Carney, C. P.; Hampton, B. S.; Ames, H. M.; Winkles, J. A.; Woodworth, G. F.; Kim, A. J. Leveraging Surface Plasmon Resonance to Dissect the Interfacial Properties of Nanoparticles: Implications for Tissue Binding and Tumor Penetration. *Nanomedicine* **2019**, *20*, 102024.
- (32) Hyun, D. C. A Polymeric Bowl for Multi-Agent Delivery. *Macromol. Rapid Commun.* **2015**, 36 (16), 1498–504.
- (33) Yoo, J.; Won, Y. Y. Phenomenology of the Initial Burst Release of Drugs from PLGA Microparticles. ACS Biomater. Sci. Eng. 2020, 6 (11), 6053–6062.